ELSEVIER

Journal of Organometallic Chemistry 550 (1998) 151–164

Journal of Organometallic Chemistry

Metallaheteroborane chemistry Part 14. [1] Synthesis of the $\{MS_2B_7\}$-cluster compounds $[9,9\text{-}(PX_3)_2\text{-}9,6,8\text{-}PtS_2B_7H_7]$ (where X = Ph or OMe), $[9,9\text{-}(PPh_3)_2\text{-}9,6,8\text{-}RhS_2B_7H_8]$ and $[5,5\text{-}(PPh_3)_2\text{-}5,6,10\text{-}RhS_2B_7H_8]$, and the $\{M_2S_2B_7\}$-cluster compound $[(PPh_3)_2HRh(PPh_3)ClRhS_2B_7H_7]$ [2]

Michael P. Murphy [a], Trevor R. Spalding [a,*], Catherine Cowey [b], John D. Kennedy [b,3], Mark Thornton-Pett. [b,4], Josef Holub [c]

[a] *Chemistry Department, University College, Cork, Ireland, UK*
[b] *School of Chemistry, University of Leeds, Leeds, LS2 9JT, England, UK*
[c] *Institute of Inorganic Chemistry, Academy of Sciences of the Czech Republic, 25068 Řež near Prague, Czech Republic*

Received 5 February 1997

Abstract

The ten-vertex $\{MS_2B_7\}$ cluster compounds $[9,9\text{-}(PPh_3)_2\text{-}9,6,8\text{-}PtS_2B_7H_7]$ **1a**, $[9,9\text{-}\{P(OMe)_3\}_2\text{-}9,6,8\text{-}PtS_2B_7H_7]$ **1c**, and $[9,9\text{-}(PPh_3)_2\text{-}9,6,8\text{-}RhS_2B_7H_8]$ **2** were synthesised in reactions between *arachno*-4,6-$S_2B_7H_9$ and the metal phosphine complexes $[Pt(PPh_3)_4]$, $[PtCl_2\{P(OMe)_3\}_2]$ and $[RhCl(PPh_3)_3]$, respectively. Heating a solution of $[9,9\text{-}(PPh_3)_2\text{-}9,6,8\text{-}RhS_2B_7H_8]$ in benzene afforded its isomer $[5,5\text{-}(PPh_3)_2\text{-}5,6,10\text{-}RhS_2B_7H_8]$ **3**. The eleven-vertex $\{M_2S_2B_7\}$ cluster compound, $[(PPh_3)_2HRh(PPh_3)ClRhS_2B_7H_7]$ **4** was synthesised in the reaction between $S_2B_7H_9$ and $[RhCl(PPh_3)_3]$ in 1:2 molar ratio, and exhibits a novel cluster structure with the metal and sulphur atoms assembled in a sequential M–S–M–S manner on the borane sub-cluster matrix. All compounds **1** to **4** were characterised by spectroscopic methods and, in the cases of **1a** and **4**, by single-crystal X-ray diffraction analysis. These observations are discussed in the light of the electronic and structural requirements of the metal units involved in metallathiaborane cluster compounds. © 1998 Elsevier Science S.A.

Keywords: Cluster compound; X-ray diffraction analysis; *Arachno*

1. Introduction

Transition-element derivatives of $\{S_2B_7\}$-based ligands are relatively rare. Two examples of ten-vertex monometalladithiaborane $\{MS_2B_7\}$ cage compounds, namely, $[9\text{-}(\eta^5\text{-Cp})\text{-}nido\text{-}9,6,8\text{-}FeS_2B_7H_9]$ [2] and $[9,9\text{-}(PMe_2Ph)_2\text{-}arachno\text{-}9,6,8\text{-}PtS_2B_7H_7]$ **1b**, [3] and three isomers with dimetallathiaborane $\{Co_2S_2B_7\}$ cages, i.e., $[8,10\text{-}(\eta^5\text{-Cp}^*)_2\text{-}nido\text{-}8,10,7,9\text{-}Co_2S_2B_7H_7]$, $[3,10\text{-}(\eta^5\text{-Cp}^*)_2\text{-}nido\text{-}3,10,7,9\text{-}Co_2S_2B_7H_7]$ and $[3,5\text{-}(\eta^5\text{-Cp}^*)_2\text{-}nido\text{-}3,5,7,9\text{-}Co_2S_2B_7H_7]$ have been reported [4,5]. Sneddon et al. have noted that, in metallaheteroboranes in general and known metallathiaboranes in particular, the metal units and sulphur atoms appear to have opposite cluster site preferences with the metal centres generally occupying sites of high coordination number and the sulphur atoms preferring low coordination numbers [4–7]. On this basis, it might therefore be expected that reactions between metal reagents and 'open' i.e., *nido*, *arachno*, or *hypho*thiaboranes which

* Corresponding author. Fax: +44-353-21-274-097.

[1] For Part 13, see Ref. [1].

[2] Dedicated to Professor Ken Wade whose outstanding work in inorganic and organometallic cluster chemistry has inspired all other researchers in this area.

[3] Also corresponding author.

[4] Also corresponding author.

have sulphur atoms at exposed low-coordination sites might afford, at least initially, unusual cage structures which might be subject to rearrangement. Here, we report (a) the syntheses of three compounds with ten-vertex $\{MS_2B_7\}$ cages, [9,9-$(PPh_3)_2$-9,6,8-$PtS_2B_7H_7$] **1a**, [9,9-$\{P(OMe)_3\}_2$-9,6,8-$PtS_2B_7H_7$] **1c** and [9,9-$(PPh_3)_2$-9,6,8-$RhS_2B_7H_8$] **2**, which have both metal and sulphur atoms in low coordination sites, (b) the thermally induced rearrangement of **2** to its isomer [5,5-$(PPh_3)_2$-5,6,10-$RhS_2B_7H_8$] **3** and (c) the synthesis of a novel cluster compound with an eleven-vertex $\{M_2S_2B_7\}$ cage, i.e., [10-Cl-8,8,10-$(PPh_3)_3$-8-H-8,10,7,9-$Rh_2S_2B_7H_7$] **4**. The last compound contains a contiguous M–S–M–S bonding sequence on the exposed face of an eleven-vertex *nido*-structured cage and two different rhodium cluster units viz. $\{RhH(PPh_3)_2\}$ and $\{RhCl(PPh_3)\}$. Compound **4** does not appear to follow either the preferred high-coordination site suggestion [4–7] for metal centres or, at first sight, simple cluster geometry/electron-counting formalisms [8,9]. It has been suggested by Adams et al. [10] and Rosair et al. [11] that, in the case of the *nido*-structured compound [8,8-$(PPh_3)_2$-8,7-$RhSB_9H_{10}$] **5** [12] and the 1,2-bis(diphenylphosphinoethane) derivative, [8-dppe-8,7-$RhSB_9H_{10}$] **5a** [10,11], the apparent *closo* electron count is actually increased by two electrons from two agostic C–H...Rh one-electron interactions. We are not convinced of this argument for **5** or **5a**, vide infra, and have similar reservations for the corresponding analysis of **4**.

2. Results and discussion

2.1. Syntheses and characterisation of $\{MS_2B_7\}$-cage compounds

2.1.1. [9,9-$(PPh_3)_2$-9,6,8-$PtS_2B_7H_7$] 1a

Reaction of *arachno*-4,6-$S_2B_7H_9$ (schematic cage structure shown in Diagram I) with $[Pt(PPh_3)_4]$ in a 1:1 molar ratio in dichloromethane at room temperature for 72 h afforded pale yellow [9,9-$(PPh_3)_2$-9,6,8-$PtS_2B_7H_7$] **1a** (53% yield). The stoichiometry of the reaction is given in Eq. (1). Compound **1a** was purified by preparative tlc followed by recrystallisation from CH_2Cl_2–hexane solution. Pale yellow crystals of **1a** which were suitable for single-crystal X-ray diffraction analysis were grown by slow diffusion of hexane into a CH_2Cl_2 solution of **1a**.

$$S_2B_7H_9 + [Pt(PPh_3)_4] \rightarrow [(PPh_3)_2PtS_2B_7H_7] + H_2\uparrow + 2PPh_3 \quad (1)$$

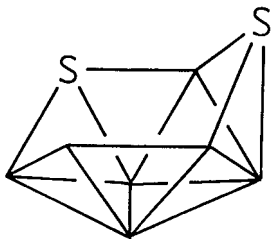

I

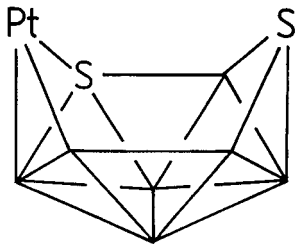

II

The X-ray analysis showed that **1a** contained a ten-vertex $\{PtS_2B_7\}$ cluster geometry as in Diagram II, with the platinum and two sulphur atoms occupying positions on the open face (Fig. 1). Important interatomic distances and angles are given in Table 1. The platinum–sulphur distance of 2.3496(10) Å in **1a** is not significantly different from that of 2.345(3) Å found in [9,9-$(PMe_2Ph)_2$-*arachno*-9,6,8-$PtS_2B_7H_7$] **1b** [3]. The two

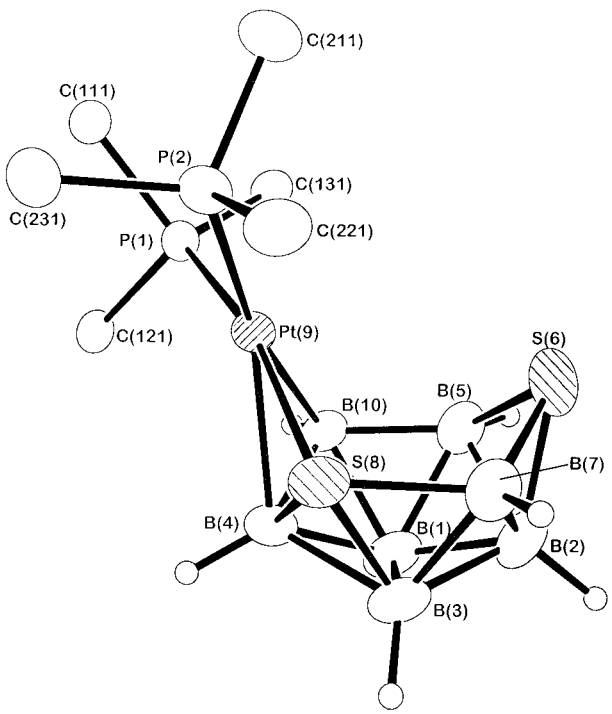

Fig. 1. ORTEP-type diagram of the crystallographically determined molecular structure of [9,9-$(PPh_3)_2$-*arachno*-9,6,8-$PtS_2B_7H_7$] **1a**.

Table 1
Important interatomic distances (Å) and angles (°) for [9,9-$(PPh_3)_2$-9,6,8-$PtS_2B_7H_7$] **1a** with e.s.d.s in parentheses

Pt(9)–B(10)	2.210(5)	Pt(9)–P(1)	2.2812(10)
Pt(9)–P(2)	2.3340(11)	Pt(9)–B(4)	2.335(5)
Pt(9)–S(8)	2.3493(11)		
B(1)–B(4)	1.728(8)	B(l)–B(3)	1.737(9)
B(l)–B(2)	1.768(9)	B(1)–B(10)	1.771(7)
B(l)–B(5)	1.804(9)	B(2)–B(7)	1.842(10)
B(2)–B(3)	1.793(9)	B(2)–S(6)	1.922(7)
B(2)–B(5)	1.861(8)	B(3)–B(7)	1.843(9)
B(3)–B(4)	1.905(8)	B(3)–S(8)	1.988(6)
B(4)–S(8)	2.152(5)	B(4)–B(10)	1.724(7)
B(5)–B(10)	1.712(7)	B(5)–S(6)	1.965(6)
B(7)–S(8)	1.919(6)	S(6)–B(7)	1.876(7)
B(10)–Pt(9)–P(1)	82.73(13)	B(1 0)–Pt(9)–P(2)	168.55(14)
P(1)–Pt(9)–P(2)	99.26(4)	B(10)–Pt(9)–B(4)	44.5(2)
P(l)–Pt(9)–B(4)	112.30(14)	P(2)–Pt(9)–B(4)	141.47(14)
B(10)–Pt(9)–S(8)	88.87(13)	P(1)–Pt(9)–S(8)	166.12(4)
P(2)–Pt(9)–S(8)	91.17(4)	B(4)–Pt(9)–S(8)	54.70(14)
B(4)–B(1)–B(3)	66.7(4)	B(4)–B(1)–B(2)	116.4(4)
B(3)–B(1)–B(2)	61.5(4)	B(4)–B(1)–B(10)	59.0(3)
B(3)–B(1)–B(10)	112.9(4)	B(2)–B(1)–B(10)	112.2(4)
B(4)–B(l)–B(5)	105.9(4)	B(3)–B(1)–B(5)	109.3(4)
B(2)–B(l)–B(5)	62.8(4)	B(10)–B(1)–B(5)	57.2(3)
B(1)–B(2)–B(3)	58.4(4)	B(1)–B(2)–B(7)	106.9(4)
B(3)–B(2)–B(7)	60.9(4)	B(l)–B(2)–B(5)	59.6(3)
B(3)–B(2)–B(5)	104.5(4)	B(7)–B(2)–B(5)	103.7(4)
B(1)–B(2)–S(6)	113.8(4)	B(3)–B(2)–S(6)	112.1(4)
B(7)–B(2)–S(6)	59.7(3)	B(5)–B(2)–S(6)	62.6(3)
B(1)–B(3)–(2)	60.1(4)	B(1)–B(3)–B(7)	108.2(4)
B(2)–B(3)–B(7)	60.9(4)	B(1)–B(3)–B(4)	56.4(3)
B(2)–B(3)–B(4)	106.8(4)	B(7)–B(3)–B(4)	110.5(4)
B(1)–B(3)–S(8)	112.5(3)	B(2)–B(3)–S(8)	111.7(4)
B(7)–B(3)–S(8)	60.0(3)	B(4)–B(3)–S(8)	67.1(2)
B(10)–B(4)–B(1)	61.7(3)	B(10)–B(4)–B(3)	107.2(4)
B(1)–B(4)–B(3)	56.9(3)	B(10)–B(4)–S(8)	110.5(3)
B(1)–B(4)–S(8)	105.6(3)	B(3)–B(4)–S(8)	58.3(2)
B(10)–B(4)–Pt(9)	63.9(2)	B(1)–B(4)–Pt(9)	114.0(3)
B(3)–B(4)–Pt(9)	111.2(3)	S(8)–B(4)–Pt(9)	62.99(14)
B(2)–B(5)–S(6)	60.2(3)	B(1 0)–B(5)–B(1)	60.4(3)
B(10)–B(5)–B(2)	110.6(4)	B(1)–B(5)–B(2)	57.7(3)
B(10)–B(5)–S(6)	122.0(4)	B(1)–B(5)–S(6)	110.2(4)
B(7)–S(6)–B(2)	58.0(3)	B(7)–S(6)–B(5)	98.6(3)
B(2)–S(6)–B(5)	57.2(3)		
B(3)–B(7)–B(2)	58.2(4)	B(3)–B(7)–5(6)	112.0(4)
B(2)–B(7)–S(6)	62.2(3)	B(3)–B(7)–S(8)	63.8 (8)
B(2)–B(7)–S(8)	112.7(4)	S(6)–B(7)–S(8)	118.0(3)
B(7)–S(8)–B(3)	56.2(3)	B(7)–S(8)–B(4)	98.1 (3)
B(3)–S(8)–B(4)	54.6(2)	B(7)–S(8)–Pt(9)	106.6(2)
B(3)–S(8)–Pt(9)	107.6(2)	B(4)–S(8)–Pt(9)	62.31(14)
B(5)–B(1 0)–B(4)	110.2(4)	B(5)–B(10)–B(1)	62.4(3)
B(4)–B(1 0)–B(1)	59.2(3)	B(5)–B(10)–Pt(9)	108.5(3)
B(4)–B(10)–Pt(9)	71.6(2)	B(1)–B(10)–Pt(9)	118.1(3)

platinum–boron distances in **1a** are Pt(9)–B(10), 2.210(5) Å and Pt(9)–B(4), 2.335(5) Å. Corresponding platinum–boron distances in compound **1b** [Pt(9)–B(10), 2.203(6) Å, Pt(9)–B(4) 2.321(6) Å] are not significantly different from those in **1a**. The fact that the platinum–sulphur and corresponding platinum–boron distances are not significantly different in **1a** and **1b** suggests that the $\{PtP_2\}$ unit bonds to the $\{S_2B_7H_7\}$ cluster in a similar manner in both compounds. This tends to be confirmed by similarities in NMR chemical shifts and fluxional properties (see below).

The sulphur–boron distances of **1a** range from 1.876(7) to 2.152(5) Å. The two sulphur atoms are positioned on the open face and separated by the B(7) atom. The close proximity of the sulphur atoms, each of which, in principle [8,9], can donate up to four electrons to the cluster bonding, affords a relatively high electron density in the {S(6)–B(7)–S(8)} region. Thus, it may not be surprising to note that the two shortest sulphur–boron distances are S(6)–B(7) at 1.876(7) A and S(8)–B(7) at 1.919(6) Å. Large variations in the boron–boron distances [1.712(7)–1.905(8) Å] are observed in **1a** but this is a common feature in boranes or heteroboranes and their metal derivatives. The longest boron–boron distances in **1a** were observed for linkages which are flanked by a sulphur atom, i.e. B(3)–B(4) at 1.905(8) Å and B(2)–B(5) at 1.861(8) Å.

The platinum–phosphorus distances in **1a** have significantly different values, i.e. Pt(9)–P(1), 2.2812(10) Å and Pt(9)–P(2), 2.3340(11) Å. These bond lengths can be compared with Pt(9)–P(1) and Pt(9)–P(2) for **1b**, [2.255(3) Å and 2.324(3) Å, respectively]. The shorter bonds in both **1a** and **1b** are for the platinum–phosphorus bonds which are *trans* to the platinum–sulphur vector.

Compound **1a** was characterised in solution with ^{11}B, ^{1}H and ^{31}P NMR spectroscopy and the results were entirely consistent with the solid-state structure. The resonances were assigned on the basis of relative intensities, relative line widths, incidences of coupling to the ^{195}Pt centre and by comparison of the shielding pattern with that of [9,9-$(PMe_2Ph)_2$-*arachno*-9,6,8-$PtS_2B_7H_7$] **1b** which has been previously reported [3].

The measured ^{11}B and $^{11}B\{^1H\}$ NMR data of **1a** recorded at 230 K in CD_2Cl_2 showed seven different boron atom resonances in a unit ratio intensity pattern indicating that the molecule did not possess any planes of symmetry and was static at 230 K. It is apparent that the B(2) resonance of **1a** is low-field while the B(1) and B(3) resonances are high-field. The higher field resonance for B(4) is possibly ascribable to localised β shielding [3] from S(6). Except for this B(4) resonance, the shielding pattern in **1a** is similar to that of the *arachno*-ten-vertex compound $[B_{10}H_{14}]^{2-}$ which has $^{11}B(2,4)$ at low-field and $^{11}B(1,3)$ at high-field. Thus it is proposed that **1a** can be described as having an *arachno* structure. This is of interest because the $\{Pt(PR_3)_2\}$ unit is usually regarded as donating two electrons to the cluster bonding [8,9] which would afford a *nido* electron count.

The ^1H NMR spectrum (CD_2Cl_2 at 230 K) consisted of phenyl resonances between $\delta(^1H)$ +7.6 and +7.2 ppm and a complex of multiplets from $\delta(^1H)$ +3.09 to

+1.18 ppm due to nine borane-cluster resonances. The ^{1}H-{^{11}B(selective)} experiments showed that each of the nine boron atoms has an *exo*-terminal hydrogen atom bound to it. No Pt–H or B–H–B proton signals were observed, in accord with the solid-state structure.

The ^{31}P {H} NMR spectrum of compound **1** at 294 K consisted of two signals each with platinum satellites and mutual coupling $^{2}J(^{31}P–^{31}P)$, consistent with the two different chemical environments. The signal from the ligand *trans* to B(7) appeared as a broader resonance [$\delta(^{31}P) = +25.4$ ppm, $^{1}J(^{195}Pt–^{31}P) = 2695$ Hz] whereas the signal of the ligand *trans* to S(5) appeared as a sharper signal with a larger coupling constant, [$\delta(^{31}P) = +33.1$ ppm, $^{1}J(^{195}Pt–^{31}P) = 4284$ Hz]. These assignments were supported by the fact that shorter platinum–phosphorus bond lengths have larger $^{1}J(^{195}Pt–^{31}P)$ coupling constants.

As the temperature at which the ^{11}B and ^{1}H spectra were recorded was raised from 230 K to 297 K, coalescence of some of the boron and proton signals was observed. The pairs of boron resonances at $\delta(^{11}B)$ +21.1 and +0.2 ppm and at $\delta(^{11}B)$ −23.4 and −34.7 ppm coalesced into two peaks which had chemical shifts of +10.2 and −27.5 ppm, respectively. Raising the temperature caused all BH proton resonances to be shifted down-field somewhat. The pairs of proton resonances at $\delta(^{1}H)$ +3.09 and +2.94 ppm and at $\delta(^{1}H)$ +1.94 and +1.18 ppm coalesced to give two peaks at δ + 3.13 and +1.65 ppm, respectively.

Similar coalescences have been observed for the previously reported PMe_2Ph analogue [9,9-$(PMe_2Ph)_2$-*arachno*-9,6,8-$PtS_2B_7H_7$] **1b** [3] and it was of interest to see if this was general for other $\{Pt(PX_3)_2\}$ units in this type of compound. We, therefore, decided to make the $P(OMe)_3$ analogue by reaction of $[PtCl_2\{P(OMe)_3\}_2]$ with $S_2B_7H_9$ in the presence of the non-nucleophilic base *N,N,N′,N′*-tetramethylnaphthalene-1,8-diamine (tmnd) (Eq. (2)).

$$S_2B_7H_9 + \left[PtCl_2\{(POMe_3)\}_2\right] + 2\,tmnd \rightarrow \left[\{P(OMe)_3\}_2PtS_2B_7H_7\right] + 2[tmndH]Cl \qquad (2)$$

Chromatographic separation thence gave pale yellow [9,9-$\{P(OMe)_3\}_2$-9,6,8-$PtS_2B_7H_7$] **1c** as an air-stable crystalline solid in 19% yield. Minor products were also present in the reaction mixture, but quantities were too small, on the reaction scale used, to permit further characterisation. The ^{11}B, ^{1}H and ^{31}P NMR behaviour of compound **1c** was analogous to that of **1a** and **1b**. At lower temperatures seven different BH(*exo*) units were distinguished with generally very similar chemical shift values to those of **1a** and **1b**, and two pairs of these coalesced at higher temperatures, with these pairs also corresponding closely to the ones in **1a** and **1b**. The NMR coalescence effects in the spectra of **1a**, **1b** and **1c** indicate fluxionality between enantiomers in solution with the platinum vertex moving to and fro between the 2,7,5 and 7,8,9 η^3-SB_2 positions of the $\{S_2B_7H_7\}$ fragment via a vertex-flip type of mechanism (Diagram III) [3]. It is notable that two discrete ^{31}P resonances are observed for all three species **1a**, **1b** and **1c** at the higher temperatures at which the $\{PtS_2B_7\}$ cage is fluxional. This indicates that the fluxional process is not associated with a general rotation of the $\{Pt(PX_3)_2\}$ moiety, but that there is a half-swing in which one phosphine ligand remains effectively *transoid* to the S(6)B(7)S(8) region, with the resultant platinum–phosphorus vector acting as a pivot for the much more marked swing of the other platinum–phosphorus vector between positions *transoid* to B(4)B(10) and B(5)B(10). The activation energy $\Delta G^{\ddagger}$ for the process in **1a**, **1b** and **1c** was determined to be 42.9 ± 0.5 kJ mol^{-1} (249 K), 44.0 ± 1.0 kJ mol^{-1} (260 K) and 39.1 ± 1.0 kJ mol^{-1} (225 K), respectively. The similarities of these $\Delta G^{\ddagger}$ values for all three species tends to confirm a similar process by a similar mechanism.

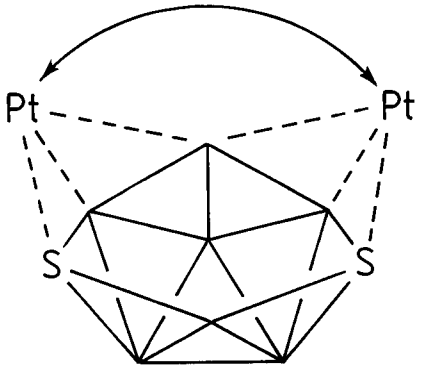

III

*2.1.2. [9,9-$(PPh_3)_2$-9,6,8-$RhS_2B_7H_8$] **2** and [5,5-$(PPh_3)_2$-5,6,9-$RhS_2B_7H_8$] **3***

The compound formulated as [9,9-$(PPh_3)_2$-9,6,8-$RhS_2B_7H_8$] **2** was synthesized by the reaction of 4,6-$S_2B_7H_9$ and an equivalent amount of $[RhCl(PPh_3)_3]$ in dichloromethane solution at room temperature for 20 min Eq. (3). Compound **2** decomposed on silica tlc plates over time (> 15 min) and therefore it was purified by dry flash chromatography. The resulting red, slightly air-sensitive compound **2** was isolated in 50% yield and stored under vacuum at 0°C. One minor product was observed from the synthetic reaction but it was formed in too small a quantity to be further characterised.

$$S_2B_7H_9 + \left[RhCl(PPh_3)_3\right] \rightarrow \left[(PPh_3)_2RhS_2B_7H_8\right] + PPh_3 + HCl \qquad (3)$$

When compound **2** was heated in refluxing benzene solution for 15 min, an isomer tentatively formulated as [5,5-$(PPh_3)_2$-5,6,10-$RhS_2B_7H_8$] **3** was formed. In $CD_3C_6D_5$ solution at 345 K, ^{11}B NMR spectroscopy showed that the conversion of **2** into **3** was quantitative with $t_{1/2}$ ca. 30 min at that temperature. Compound **3** was purified by dry flash chromatography since, like **2**, it decomposed on silica over time. Compound **3** was isolated as a red, slightly air-sensitive solid in 12% yield and stored under vacuum at 0°C. Both **2** and **3** were characterised by ^{11}B, ^{1}H and ^{31}P NMR spectroscopy. The parallels in synthetic route Eqs. (2) and (3) and in transition-element character, together with general parallels in NMR behaviour suggest compound **2** has similar electronic structure to compounds **1a**, **1b**, and **1c**, i.e. **2** may be formulated as [9,9-$(PPh_3)_2$-*arachno*-9,6,8-$RhS_2B_7H_8$], the principal difference being the presence of a bridging hydrogen atom at B(5)–B(10) which is in the typical *arachno* ten-vertex position as exemplified by $[B_{10}H_{14}]^2$. This appears to induce a higher ^{11}B shielding at the BH(5) and BH(10) positions in **2** at the expense of lower shieldings at the BH(1) and BH(2) positions. The ^{31}P NMR spectrum exhibited two mutually coupled resonances also coupled to ^{103}Rh with magnitudes indicating a *cis*-{$Rh(PPh_3)_2$} unit in the cluster. The proposed cluster structure of **2** is in Diagram IV. As with compounds **1a**, **b** and **c** there is an incompatibility of this *arachno*-type formulation with a formal *nido* electron count for **2**. In this context, **2** has similarities to the eleven-vertex species [$(PPh_3)_2$-$RhSB_9H_{10}$] [12] and [$(PPh_3)_2RhC_2B_8H_{11}$] [13] which can adopt open *nido* structures in spite of having formal *closo* electron counts. However, in the rhodacarborane case, there is equilibration with a *closo* structured form of [$(PPh_3)_2RhC_2B_8H_{11}$] which is compatible with its electron count, whereas with **2** there is no equilibration involving a *nido*-type species with a terminal Rh–H bond. Unlike the platinum analogues **1a**, **b** and **c**, the rhodium species **2** is not fluxional. Presumably the bridging hydrogen atom blocks any attempt by the rhodium atom at traversing the cluster face in a mechanism analogous to that in Diagram III. Again this contrasts with [$(PPh_3)_2RhC_2B_8H_{11}$], in which the BHB hydrogen atom actually participates in the equilibration process and forms a Rh–H bond in the *closo* form of [$(PPh_3)_2RhC_2B_8H_{11}$] [13].

Although the heating of **2** does not reveal a fluxionality, it does reveal a quantitative conversion to an isomer, compound **3**, which is tentatively proposed to have the [5,5-$(PPh_3)_2$-5,6,10-$RhS_2B_7H_8$] formulation, Diagram V. This would derive mechanistically from compound **2** by a vertex-swing of the S(6) atom of **2**. However, other structures such as the [5,5-$(PPh_3)_2$-5,6,9-$RhS_2B_7H_8$] formulation of Diagram VI, or with the {$Rh(PPh_3)_2$} unit moved off the open face, would not be incompatible with the NMR data and present knowledge of ^{11}B shielding factors. A 5-{$Rh(PPh_3)_2$} positioning is perhaps suggested by the significant shift to lower field of one of the ^{11}B resonances, that at $\delta(^{11}B)$ +17.7 or +19.3 in compound **3**, 6-metalla to 5-metalla conversions in this ten-vertex shape often being associated with a similar low-field shift [14].

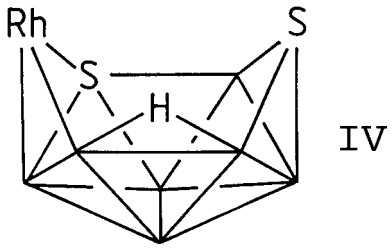

IV

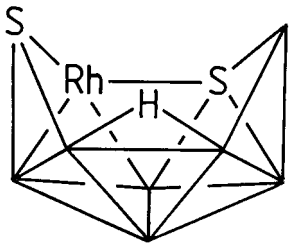

V

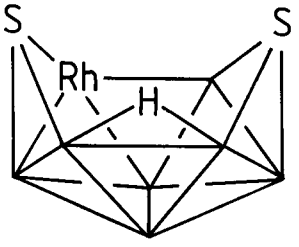

VI

*2.1.3. Syntheses and characterisation of the dimetallic species [8,8,10-$(PPh_3)_3$-8-H-10-Cl-8,10,9,7-$Rh_2S_2B_7H_8$] **4***

The reaction between [9,9-$(PPh_3)_2$-9,6,8-$RhS_2B_7H_8$] **2** and [$RhCl(PPh_3)_3$] in a 1:1 molar ratio in dichloromethane solution at room temperature for 60 h affords air-stable, orange [$(PPh_3)_2HRh(PPh_3)Cl$-$RhS_2B_7H_7$] **4** in 23% yield. Alternatively, a one-pot reaction of *arachno*-4,6-$S_2B_7H_9$ with [$RhCl(PPh_3)_3$] in a 1:2 molar ratio in dichloromethane for 72 h at room temperature afforded compound **4** in the higher yield of 34% Eq. (4). A minor product from this reaction was identified as **2**. Compound **4** was purified in both preparations by preparative tlc followed by recrystallisation from CH_2Cl_2–hexane solution.

$$2[RhCl(PPh_3)_3] + S_2B_7H_9 \rightarrow [(PPh_3)_2HRh(PPh_3)ClRhS_2B_7H_7] + (2PPh_3)_2 + HCl) \quad (4)$$

The molecular structure of compound **4** was established by a single crystal X-ray diffraction study. Suitable crystals were grown by slow diffusion of a layer of hexane into a solution of **4** in CH_2Cl_2. The analysis showed the gross cage geometry to be that of an eleven-vertex *nido* cluster with a five-membered $\{Rh_2S_2B\}$ open face, see Fig. 2 and Diagram VII. Important interatomic distances and angles in **4** are given in Table 2.

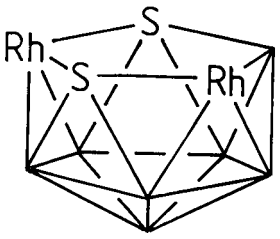

VII

The longest rhodium–sulphur distance in **4** is Rh(8)–S(9), 2.4422(10) Å. This vector is *trans* to the rhodium hydride bond (Fig. 2). The other rhodium sulphur distance involving Rh(8) is 2.3975(10) Å to S(7). Comparison may be made with the structure of $[8,8\text{-}(PPh_3)_2\text{-}8\text{-}H\text{-}nido\text{-}8,7,9\text{-}RhS_2B_8H_8]$ **6** [15]. Of the two rhodium–sulphur distances in **6** that *trans* to the rhodium hydride vector, 2.4304(5) Å, is significantly longer than that *cis* to it, 2.3567(5) Å [15]. A rhodium–sulphur distance of 2.447(3) Å which is similar to Rh(8)–S(9) in **4** has been reported for the rhodacarbathiaborane $[8,8\text{-}(PPh_3)_2\text{-}8\text{-}H\text{-}nido\text{-}8,7,9\text{-}RhCSB_8H_{10}]$ [16] and again the rhodium–sulphur linkage is *trans* to a rhodium hydride vector. The Rh(10)–S(9) distance in **4**, 2.3409(10) Å is shorter than any previously found in phosphine-ligated rhodathiaboranes including $[8,8\text{-}(PPh_3)_2\text{-}8,7\text{-}RhSB_9H_{10}]$ **5**, 2.3769(9) Å [12].

The chlorine atom Cl(1) is attached to the coordinatively unsaturated rhodium atom Rh(10) at a distance of 2.3710(10) Å. This bond is longer than the rhodium–chlorine terminal bond, 2.356(2) Å, in $[2,3\text{-}(PPh_3)_2\text{-}3\text{-}Cl\text{-}\mu\text{-}2;3\text{-}Cl\text{-}2\text{-}(Ph_2PC_6H_4)\text{-}closo\text{-}2,3,1\text{-}Rh_2S_9H_8]$, which is the only previously reported rhodathiaborane to contain such a bond [12].

The rhodium–boron distances in **4** range from 2.076(4) to 2.255(4) Å. This range is considerably larger than that found in either **5** or **6**, i.e. 2.146(3) to 2.242(4) and 2.240(2) to 2.242(2) Å, respectively. The sulphur–boron distances in **4** vary from 1.964(4) to 2.016(4) A whereas a larger range, 1.908(4) to 2.035(4) Å, is observed in **5**. It is noteworthy that the sulphur–boron and rhodium–boron connectivities in **4** that are flanked by a rhodium or a sulphur atom, e.g. S(7)–B(3) and Rh(8)–B(3), are considerably longer than those that are flanked by a boron atom. A large range in the interboron distances in **4** is apparent, from 1.734(6) for B(2)–B(6) to 1.942(6) Å for B(4)–B(5), but this is not unexpected for metallaboranes.

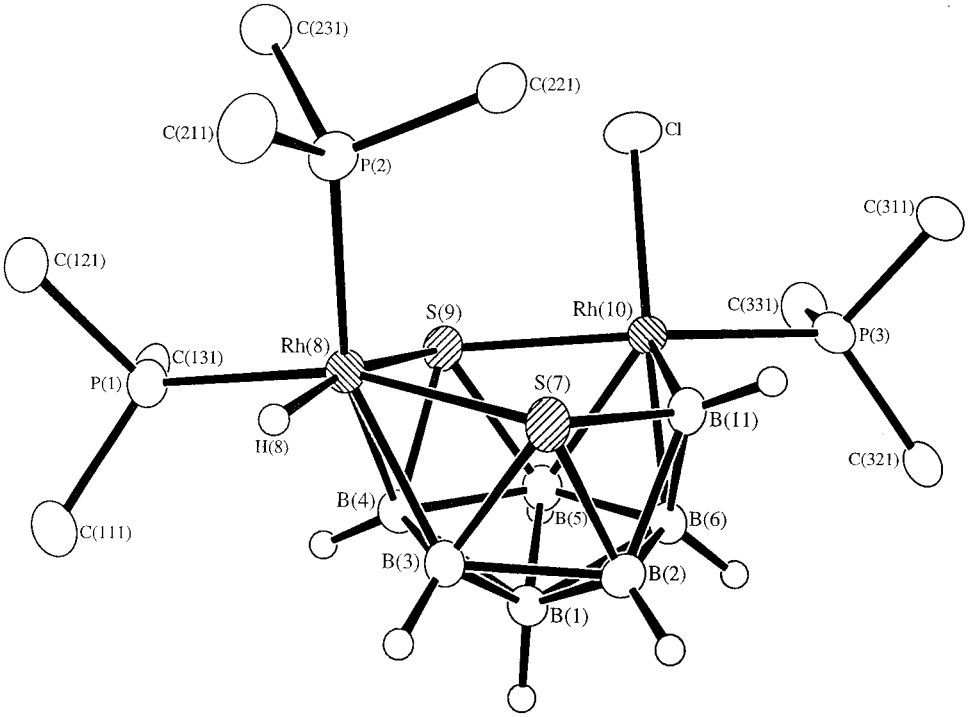

Fig. 2. ORTEP-type diagram of the crystallographically determined molecular structure of $[(PPh_3)_2HRh(PPh_3)ClRhS_2B_7H_7]$ **4**, with selected *P*-organyl atoms omitted for clarity.

Table 2
Important interatomic distances (Å) and angles (°) for [8,8,10-$(PPh_3)_3$-8-H-10-Cl-8,10,9,7-$Rh_2S_2B_7H_7$] **4** with e.s.d.s in parentheses

Rh(8)–B (4)	2.248(4)	Rh(8)–B(3)	2.255(4)
Rh(8)–P(1)	2.2967(10)	Rh(8)–P(2)	2.3696(10)
Rh(8)–S(7)	2.3975(10)	Rh(8)–S(9)	2.4422(10)
Rh(8)–H(8)	1.55(5)		
Rh(10)–B(11)	2.076(4)	Rh(10)–B(5)	2.157(4)
Rh(10)–B(6)	2.180(4)	Rh(10)–P(3)	2.2886(10)
Rh(10)–S(9)	2.3409(10)	Rh(10)–Cl	2.3710(10)
B(1)–B(2)	1.751(6)	B(1)–B(3)	1.772(6)
B(1)–B(5)	1.776(6)	B(1)–B(4)	1.781(6)
B(1)–B(6)	1.808(6)	B(2)–B(11)	1.867(6)
B(2)–B(6)	1.734(6)	B(2)–S(7)	2.010(4)
B(2)–B(3)	1.879(6)	B(3)–B(4)	1.813(6)
B(3)–S(7)	2.016(4)	B(4)–S(9)	1.987(4)
B(4)–B(5)	1.942(6)	B(5)–B(6)	1.788(6)
B(5)–S(9)	1.994(4)	S(7)–B(11)	1.964(4)
B(6)–B(11)	1.765(6)		
B(4)–Rh(8)–B(3)	47.5(2)	B(4)–Rh(8)–P(1)	87.09(11)
B(3)–Rh(8)–P(1)	113.84(11)	B(4)–Rh(8)–P(2)	158.35(11)
B(3)–Rh(8)–P(2)	141.26(11)	P(1)–Rh(8)–P(2)	99.79(4)
B(4)–Rh(8)–S(7)	86.80(11)	B(3)–Rh(8)–S(7)	51.25(11)
P(1)–Rh(8)–S(7)	162.42(3)	P(2)–Rh(8)–S(7)	91.87(3)
B(4)–Rh(8)–S(9)	49.92(11)	B(3)–Rh(8)–S(9)	87.36(11)
P(1)–Rh(8)–S(9)	95.61(3)	P(2)–Rh(8)–S(9)	108.68(4)
S(7)–Rh(8)–S(9)	93.01(3)		
B(11)–Rh(10)–B(5)	87.1(2)	B(11)–Rh(10)–B(6)	48.9(2)
B(5)–Rh(10)–B(6)	48.7(2)	B(11)–Rh(10)–PI(3)	95.86(11)
B(5)–Rh(10)–P(3)	119.34(11)	B(6)–Rh(10)–PI(3)	90.47(11)
B(11)–Rh(10)–S(9)	99.04(11)	R(5)–Rh(10)–S(9)	52.43(11)
B(6)–Rh(10)–S(9)	92.13(11)	P(3)–Rh(10)–S(9)	162.30(3)
B(11)–Rh(10)–Cl	127.45(12)	B(5)–Rh(10)–C1	134.65(11)
B(6)–Rh(10)–Cl	176.18(11)	P(3)–Rh(10)–C1	88.74(4)
S(9)–Rh(10)–Cl	89.75(4)	C(131)–P(1)–Rh(8)	114.98(12)
C(121)–P(1)–Rh(8)	116.32(12)	C(111)–P(1)–Rh(8)	116.50(13)
C(221)–P(2)–Rh(8)	118.18(14)	C(231)–P(2)–Rh(8)	116.54(13)
C(321)–P(3)–Rh(10)	119.30(12)	C(211)–P(2)–Rh(8)	111.84(12)
C(331)–P(3)–Rh(10)	101.31(13)	C(311)–P(3)–Rh(10)	120.31(12)
B(2)–B(1)–B(3)	64.4(2)	B(2)–B(1)–B(5)	109.7(3)
B(3)–B(1)–B(5)	114.2(3)	B(2)–B(1)–B(4)	115.0(3)
B(3)–B(1)–B(4)	61.4(2)	B(5)–B(1)–B(4)	66.2(2)
B(2)–B(1)–B(6)	58.3(2)	B(3)–B(1)–B(6)	111.(2)
B(5)–B(1)–B(6)	59.8(2)	B(4)–B(1)–B(6)	114.2(3)
B(6)–B(2)–B(3)	62.5(2)	B(6)–B(2)–B(1)	58.6(2)
B(1)–B(2)–B(11)	107.4(3)	B(6)–B(2)–B(3)	109.7(3)
B(1)–B(2)–B(3)	58.3(2)	B(11)–B(2)–S(7)	108.4(3)
B(6)–B(2)–B(3)	110.3(2)	B(1)–B(2)–S(7)	109.7(2)
B(11)–B(2)–S(7)	60.7(2)	B(3)–B(2)–S(7)	62.3(2)
B(1)–B(3)–B(4)	59.6(2)	B(1)–B(3)–B(2)	57.2(2)
B(4)–B(3)–B(2)	107.6(3)	B(1)–B(3)–S(7)	108.6(2)
B(4)–B(3)–S(7)	112.9(2)	B(2)–B(3)–S(7)	62.0(2)
B(1)–B(3)–Rh(8)	118.3(3)	B(4)–B(3)–Rh(8)	66.1(2)
B(2)–B(3)–Rh(8)	121.4(2)	S(7)–B(3)–Rh(8)	68.02(13)
B(1)–B(4)–B(3)	59.1(2)	B(1)–B(4)–B(5)	56.8(2)
B(3)–B(4)–B(5)	104.9(3)	B(1)–B(4)–S(9)	111.2(2)
B(3)–B(4)–S(9)	117.3(2)	B(5)–B(4)–S(9)	61.0(2)
B(1)–B(4)–Rh(8)	118.2(2)	B(3)–B(4)–Rh(8)	66.5(2)
R(5)–B(4)–Rh(8)	118.2(2)	S(9)–B(4)–Rh(8)	70.11(13)
B(1)–B(5)–B(6)	61.0(2)	B(1)–B(5)–B(4)	57.0(2)
B(6)–B(5)–B(4)	107.7(3)	B(1)–B(5)–S(9)	111.1(2)
B(6)–B(5)–S(9)	118.9(2)	B(4)–B(5)–S(9)	60.6(2)
B(1)–B(5)–Rh(10)	117.6(2)	B(6)–B(5)–Rh(10)	66.3(2)
B(4)–B(5)–Rh(10)	116.2(2)	S(9)–B(5)–Rh(10)	68.54(13)
B(2)–B(6)–B(11)	64.5(2)	B(2)–B(6)–B(5)	109.9(3)
B(11)–B(6)–B(5)	110.3(3)	B(2)–B(6)–B(1)	59.2(2)

Table 2 (continued)

B(11)–B(6)–B(1)	109.4(3)	B(5)–B(6)–B(1)	59.2(2)
B(2)–B(6)–Rh(10)	118.9(3)	B(11)–B(6)–Rh(10)	62.5(2)
B(5)–B(6)–Rh(10)	65.0(2)	B(1)–B(6)–Rh(10)	115.0(2)
B(11)–S(7)–B(2)	56.0(2)	B(11)–S(7)–B(3)	99.5(2)
B(2)–S(7)–B(3)	55.6(2)	B(11)–S(7)–Rh(8)	113.25(12)
B(2)–S(7)–Rh(8)	109.64(13)	B(3)–S(7)–Rh(8)	60.72(12)
B(4)–S(9)–B(5)	58.4(2)	B(4)–S(9)–Rh(10)	106.83(12)
B(5)–S(9)–Rh(10)	59.04(12)	B(4)–S(9)–Rh(8)	59.97(12)
B(5)–S(9)–Rh(8)	108.08(13)	Rh(10)–S(9)–Rh(8)	111.67(4)
B(6)–B(11)–B(2)	56.9(2)	B(6)–B(11)–S(7)	111.1(2)
B(2)–B(11)–S(7)	63.2(2)	B(6)–B(11)–Rh(10)	68.6(2)
B(2)–B(11)–Rh(10)	117.8(2)	S(7)–B(11)–Rh(10)	119.2(2)

The rhodium–phosphorus distances Rh(8)–P(1) and Rh(10)–P(3) are 2.2967(10) and 2.2886(10) Å. These bonds are *trans* to Rh–S interactions and are considerably shorter than the Rh(8)–P(2) distance of 2.3696(10) Å. Similar effects were observed in [8,8-$(PPh_3)_2$-8-H-*nido*-8,7,9-$RhS_2B_8H_8$] **6** and [8,8-$(PPh_3)_2$-8,7-$RhSB_9H_{10}$] **5**, where the rhodium–phosphorus vector *trans* to the sulphur atom was shorter than the second rhodium–phosphorus distance, i.e. respectively 2.3103(5) and 2.3604(5) Å for **6** [15] and 2.4197(5) and 2.2906(5) Å for **5** [12].

The ^{11}B, ^{1}H and ^{31}P NMR parameters measured for compound **4** were consistent with the solid-state structure. There were seven boron resonances in the region $\delta(^{11}B)$ +17.6 to −25.2 ppm The proton NMR spectrum consisted of phenyl resonances between δ +7.68 and +6.94 ppm and a complex of multiplets from $\delta(^{1}H)$ +5.48 to +1.31 ppm due to seven BH resonances. ^{1}H–{^{11}B(selective)} spectroscopy showed that all seven boron atoms had *exo* hydrogen atoms bound to them. There was an additional resonance at $\delta(^{1}H)$ −11.19 p.p.m with $^{1}J(^{103}Rh-^{1}H)$ ca. 16 Hz. This may be compared to the Rh–H resonance in [8,8-$(PPh_3)_2$-8-H-*nido*-8,7,9-$RhCSB_8H_{10}$] at $\delta(^{1}H)$ −11.85 ppm [$^{1}J(^{103}Rh-^{1}H) = 34$ Hz] [16].

The ^{31}P NMR spectrum of **4** showed three resonances in a 1:1:1 relative intensity ratio. Two of these are at $\delta(^{31}P)$ +46.3 ppm [$^{1}J(^{103}Rh-^{31}P)$ 143 Hz] and +33.7 ppm [$^{1}J(^{103}Rh-^{31}P)$ 117 Hz]. Both of these display as doublets of doublets with a mutual coupling constant $^{2}J(^{31}P-^{31}P)$ of 21 ± 4 Hz, which indicated that both of these phosphines are bonded to the same rhodium atom, Rh(8). The third resonance occurred at $\delta(^{31}P)$ +34.1 ppm [$^{1}J(^{103}Rh-^{31}P)$ 149 Hz] but showed no coupling $^{2}J(^{31}P-^{31}P)$ suggesting that this phosphine is the one bonded to rhodium atom Rh(10).

The cluster structure of **4** is based on a conventional *nido*-type eleven-vertex geometry with the S–Rh–S–Rh sequence as part of the open face, i.e. {S-$RhH(PPh_3)_2$-S-$Rh(PPh_3)Cl$}. The fact that compound **4** contains two different metal units, {$Rh(PR_3)_2H$} and {$RhCl(PR_3)$}, is of interest. The {$Rh(PR_3)_2H$} unit is commonly found in rhodaheteroboranes, including carboranes [17–20] and selena- and telluraboranes [21] and it formally donates two electrons to cluster bonding. The {$RhCl(PR_3)$} unit is, by contrast, an unusual moiety in rhodaheteroboranes and formally donates zero electrons to cluster bonding, i.e., equivalent to $\{BH_2\}^{3+}$. Hence, compound **4** has a formal *closo* electron count but a *nido* structure and thereby apparently contravenes Wadian electron-counting rules [8,9]. A similar anomaly exists in [8,8-$(PPh_3)_2$-8,7-$RhSB_9H_{10}$] **5** [12] and a related *nido/arachno* anomaly exists in **1a**, **b** and **c**. Here, it is noteworthy that the only {$M_2S_2B_7$} cluster compounds previously reported, i.e., three isomers containing the {$Co_2S_2B_7$} cage, [8,10-(η^5-Cp^*)$_2$-*nido*-8,10,7,9-$Co_2S_2B_7H_7$], [3,10-(η^5-Cp^*)$_2$-*nido*-3,10,7,9-$Co_2S_2B_7H_7$] and [3,5-(η^5-Cp^*)$_2$-*nido*-3,5,7,9-$Co_2S_2B_7H_7$] obey the established electron-counting rules and adopt eleven-vertex *nido* cage structures based on an icosahedron with one vertex missing [4,5]. The evidence for the {$Co_2S_2B_7$} compounds was obtained from their ^{11}B NMR spectra and a preliminary single-crystal X-ray diffraction study of the 8,10,7,9-{Co_2S_2} isomer.

The overall structure of **4** can be interpreted as unusual, with the apparent deficiency of one pair of electrons in the cluster bonding in compound **4** arising because of the formally sixteen-electron transition-element centre, i.e. {$RhCl(PPh_3)$}, whereas application of Wade's rules often presumes eighteen-electron transition-element behaviour. In our opinion there is an important general point here which relates to the evaluation of the formal electron count at metal atoms in clusters. The point is that, in formal electron-counting terms, some transition-element centres may prefer sixteen-electron configurations rather than eighteen-electron ones when bonding in metallaborane or metallahetroborane cluster compounds just as they can do in non-borane ligated compounds. We would suggest that

this is observed quite commonly in borane-containing compounds of palladium, platinum, rhodium and similar elements when the transition-element has two *exo*-cluster ligands. Hence, the common approach to electron counting in these compounds often needs to be modified to be in accord with the observed cluster geometry. However, the alternative explanation of the unexpected structure/electron-count of compound **4** which is based on the suggestion that two extra cluster electrons may be provided from two C–H...Rh agostic interactions [10,11] is worth consideration. The agostic interactions could possibly arise from the triphenylphosphine CH units if they were located in suitable positions [10,11]. The two shortest C–H...Rh distances in the three crystallographically independent molecules of [8-dppe-8,7-$RhSB_9H_{10}$] **5a** [10,11] which were observed in two dichloromethane solvates of **5a**, i.e. **5a**, $2CH_2Cl_2$ and **5a**. 1/2 CH_2Cl_2 were 3.254(11) and 2.742(12) Å, 3.119(14) and 2.849(10) Å, and 3.174 and 2.809 Å, respectively. In compound **4**, the two closest C–H...Rh(10) distances are 3.189 and 3.394 Å and involve H(336) and H(316), respectively. However, for the rhodium atom with higher coordination, the related C–H...Rh(8) distances fall between the C–H...Rh(10) distances at 3.251 and 3.260 Å and involve H(112) and H(226), respectively. It seems unlikely that both rhodium atoms have gained two extra electrons from two, one-electron, agostic C–H...Rh bonds. If this were so, it would lead to an *arachno* electron count. Furthermore, it is noteworthy that some of the B–H...Rh distances are shorter than the C–H...Rh ones above. The two shortest B–H...Rh distances to Rh(10) are 2.77(4) and 2.83(4) Å to H(11) and H(6), respectively, and those to Rh(8) are 2.91(4) and 3.02(4) Å to H(3) and H(4) respectively. A similar observation about the proximity of B–H...Rh atoms has been made elsewhere in discussion of the structure of [μ-9,10-(SMe)-8-(η^4-C_5Me_5H)-*nido*-8,7-$RhSB_9H_9$] [22]. At this stage, we are unconvinced of the agostic bonding explanation of the structures of **4**, **5** and **5a** and we intend to address this problem in more detail in later publications.

The origins of the M–S–M–S sequence in **4** are of interest. The formation of compound **4** must involve a cluster skeletal rearrangement which may be related to the **2** to **3** conversion mentioned above. Thus the reaction possibly involves the initial formation of **2** (schematic structure IV) followed by a vertex 'flip' to yield the desired precursor geometry V, i.e. that proposed for compound **3**, before the addition of the second rhodium unit. Notwithstanding the details of the intimate mechanism, it is apparent that with these types of metal centres there is a clear driving force for facile metal–sulphur grouping and thence $\{M_2S_2\}$ subcluster self-assembly on the boron hydride framework. It is likely that this depends critically on the particular metal unit being added and the relative affinities of metal units for sulphur *vs.* boron binding. Thus, choice of metal unit and reaction conditions will permit some structural 'tailoring' of these types of systems in the future.

3. Experimental

General methods for the syntheses and spectroscopic characterisation of compounds have been described in previous Parts in this series [1]. The compound *arachno*-4,6-$S_2B_7H_9$ was prepared according to the literature method [23]. The complexes, [$RhCl(PPh_3)_3$] [24], [$Pt(PPh_3)_4$] [25] and [$PtCl_2\{(POMe_3)\}_2$] [26] were synthesized as described in the literature from [$RhCl_3 \cdot xH_2O$] and $K_2[PtCl_4]$, respectively. NMR chemical shifts $\delta(^{11}B)$, $\delta(^{31}P)$ and $\delta(^{1}H)$ are given in ppm to high frequency (low field) of BF_3OEt_2, 85% H_3PO_4 and $SiMe_4$, respectively.

3.1. [9,9-$(PPh_3)_2$-9,6,8-$PtS_2B_7H_7$] **1a**

A solution of [$Pt(PPh_3)_4$] (0.166 g, 0.134 mmol) in dichloromethane (15 cm^3) was added to a solution of *arachno*-4,6-$S_2B_7H_9$ (0.018 g, 0.134 mmol) in dichloromethane (10 cm^3). The yellow reaction mixture was stirred at room temperature for 72 h. The solution was concentrated under reduced pressure and subjected to preparative tlc (CH_2Cl_2–heptane) (8:2). The single major yellow band was extracted into dichloromethane. Recrystallisation from CH_2Cl_2–hexane afforded pale yellow block crystals of [9,9-$(PPh_3)_2$-9,6,8-$PtS_2B_7H_7$] **1a** (0.062 g, 53.1%). (Found: C, 49.9; H, 4.3. $C_{36}H_{37}B_7P_2PtS_2$ requires C, 49.85; H, 4.65%). IR: ν_{max} (KBr) 2555(m), 2530(s), 2490(s) (BH) cm^{-1}. ^{11}B and ^{1}H NMR data (CD_2Cl_2 230 K) ordered as assignment $\delta(^{11}B)$[$\delta(^{1}H)$ of directly attached proton]: BH(4) +21.1 [+3.09], BH(5) +0.2 [+2.94], BH(10) −3.0 [+1.98], BH(7) −6.0 [+2.72], BH(1) −18.7 [+1.42], BH(2) −23.4 [+1.94], BH(3) −33.8 [+1.18]; and at 297 K ordered as assignment $\delta(^{11}B)$, multiplicity, [$\delta(^{1}H)$ of directly attached proton]: BH(4,5) +10.2, 2, [+3.13], BH(10) −2.5, 1, [+2.16], BH(7) −3.6, 1, [+2.82], BH(1) −16.3, 1, [+1.56], BH(2,3) −27.5, 2, [+1.65]. Additionally, $\delta(^{31}P)$ (CD_2Cl_2, 294 K) +33.1 [$^1J(^{195}Pt–^{31}P)$ 4284 Hz] and +25.4 [$^1J(^{195}Pt–^{31}P)$ 2695 Hz] with $^2J(^{31}P–^{31}P)$ 2112 Hz. (For X-ray Diffraction analysis of **1a**, see Section 3.6 and Table 3).

3.2. [9,9-$\{P(OMe)_3\}_2$-9,6,8-$PtS_2B_7H_7$] **1c**

A solution of *arachno*-4,6-$S_2B_7H_9$ (0.024 g, 0.160 mmol) and tetramethylnaphthalenediamine (tmnd; 0.092 g, 0.430 mmol) in dichloromethane (20 cm^3) was stirred for 10 min and then [$PtCl_2\{(POMe_3)\}_2$] (0.100 g, 0.195 mmol) added. Stirring was continued for 24 h. The mixture was then filtered through silica (tlc-grade, ca. 3

Table 3
Crystal data and details of refinement[a]

Empirical Formula	$C_{36}H_{37}B_7P_2PtS_2$	$C_{54}H_{53}B_7ClP_3RhS_2 \cdot CH_2Cl_2$
Formula weight	866.48	1262.52[b]
a/Å	11.l943(8)	12.254(2)
b/Å	11.4722(10)	12.662(2)
c/Å	16.027(14)	19.542(2)
α/°	89.468(7)	7.006(11)
β/°	89.776(7)	77.835(9)
γ/°	64.367(5)	87.237(10)
υ/Å	3736.5(3)	2805.9(8)
D_c/M gm^{-3}	1.551	1.492
μ/mm^{-1}	9.124	0.928
F(000)	856	1276
Max, min transmission factors	0.318, 0.239	0.837, 0.742
Crystal Size/mm	0.65 × 0.34 × 0.31	0.48 × 0.35 × 0.26
hkl ranges	−28,13; −13,13; −7,19	−14,14; −14,15; −14,23
Reflections collected	6553	10 039
Independent reflections, p	6516	9878
Reflections with $F_0^2 > 2F_0^2$	5830	7697
Weighing scheme parameters a, b[c]	0.0368, 1.6312	0.0385, 49 892
Data, restraints, parameters (n)	6516, 465, 461	9878, 45, 699
Goodness of fit on F^2, s[d]	1.163	1.024
R_1[e]	0.0259	0.0541
wR_2[f]	0.0689	0.0859
Largest diff. map peak and hole/e Å^{-3}	0.625, −0.810	0.524, −0.539

[a]Common to both structures: crystal system triclinic, space group PT, $Z = 2$.
[b]Includes solvate molecule.
[c]$w = 1/[\sigma^2(F_o^2) + aP^2 + bP)]$, where P $(F_o^2 + 2F_c^2)/3$.
[d]$S = [\Sigma[w(F_o^2 - F_c^2)^2]/(n-p)]^{1/2}$
[e]$R_1 = [\Sigma||F_o|F_c||]/\Sigma|F_o|$ for $I > 26(I)$.
[f]$wR_2 = \{\Sigma[w(F_o^2 - F_c^2)^2]/\Sigma(F_0^2)^2]\}^{1/2}$ for all data.

g) with the aid of additional dichloromethane (50 cm^3). The combined filtrates were concentrated under reduced pressure and the residue subjected to repeated preparative tlc (silica gel G, Fluka type GF_{254}: eluents CH_2Cl_2 and Et_2O) to yield two pale yellow components R_f (100% CH_2Cl_2 eluent) ca. 0.25 and 0.50. The small yield of the component with R_f 0.25 prohibited further characterisation. The component with R_f 0.50 was identified as [9,9-{P(OMe)$_3$}$_2$-9,6,8-$PtS_2B_7H_7$] **1c** (0.023 g, 19%) by NMR spectroscopy and mass spectrometry. NMR data for **1c** ordered as assignment $\delta(^{11}B)$ [$\delta(^1H)$ of directly attached proton] (a) 193 K, CD_2Cl_2, BH(4) +22 [+3.03], BH(5) +3 [+2.91], BH(7) −5 [+3.24], BH(10) −12 [+2.22], BH(1) −23 [+1.50], BH(2) −25 [+1.82], BH(3) −35 [+1.40], (b) 294 − 297 K, CD_2Cl_2, BH(4,5) +9.4 [+3.06], BH(7) −5.9 [+3.31], BH(10) −12.8 [+2.33], BH(1) − 21.9 [+1.64, $^3J(^{195}Pt-^1H)$ ca. 45 Hz], BH(2,3) −30.0 [+1.68, $^{314}J(^{195}Pt-^1H)$ ca. 40 Hz]; at 128 MHz the coalescence temperature for $\delta(^{11}B)(4)$ and $\delta(^{11}B)(5)$ was 233 K, and for $\delta(^{11}B)(2)$ and $\delta(^{11}B)(3)$ 218 K, giving values of $\Delta G^{\neq}$ of 39.9 ± 1.0 and 39.1 kJ mol^{-1}, respectively. $\delta(^1H)$(P(OMe)$_3$), $CDCl_3$ 294 K +3.64 and +3.84 both $^3J(^{31}P-^1H)$ 13 Hz, $\delta(^{31}P)$ $CDCl_3$, 223 K +116.6 (sharp) $^1J(^{195}Pt-^{31}P)$ 6412 Hz and +132.8 (broader) $^1J(^{195}Pt-^{31}P)$ 4286 Hz; with $^2J(^{31}P-^{31}P)$ 53 Hz. The mass spectrum (70 eV EI) gave a high mass cut-off at the m/e value corresponding to the highest isotopomer of the molecular formula.

3.3. [9,9-(PPh$_3$)$_2$-9,6,8-$RhS_2B_7H_8$] 2

A solution of [$RhCl(PPh_3)_3$] (0.108 g, 0.117 mmol) in dichloromethane (5 cm^3) was added to a solution of *arachno*-4,6-$S_2B_7H_9$ (0.017 g, 0.117 mmol) in dichloromethane (2 cm^3). The orange reaction mixture was stirred for 20 min at room temperature. The reaction mixture was then filtered through a sintered glass crucible (No. 3), containing tlc-grade silica (7.0 g), using dichloromethane (10 cm^3) as eluent. The filtrate was concentrated under reduced pressure to yield a solid crude product which was washed with hexane (3 × 5 cm^3) to afford red, slightly air-sensitive [9,9-(PPh$_3$)$_2$-9,6,8-$RhS_2B_7H_8$] **2** (0.042 g, 50.1%) formulated as such as described in the text. (Found: C, 55.9; H, 5.1; S, 8.2. $C_{36}H_{38}B_7P_2RhS_2$ requires C, 55.75; H, 4.95; S, 8.3%). IR: ν_{max} (KBr) 2578(s), 2577(s), 2545(s), 2527(s), 2490(s) (BH) cm^{-1}. ^{11}B and ^1H NMR data for

2, (CD_2Cl_2, 297 K) ordered as $\delta(^{11}B)$[$\delta(^1H)$ of directly attached proton]: +21.9 [+4.45], +0.5 [+3.22], −6.5 [+2.43], −12.6 [+2.69], −16.3 [+2.42], −20.8 [+1.10], and −38.1 [+0.53]; $\delta(^1H)(\mu H)$ +1.01 (associated principally with $\delta(^{11}B)$ +0.5 and −20.8); $\delta(^{31}P)$ 219 K, $CDCl_3$) (a) +46.8 and (b) +29.5, $^1J(^{103}Rh-^{31}P_a)$ 189 Hz, $^1J(^{103}Rh-^{31}P_b)$ 156 Hz, and $^2J(^{31}P_a-^{31}P_b)$ 39 Hz. Compare with [9,9-$(PMe_2Ph)_2$-*arachno*-9,6,8-$PtS_2B_7H_7$] **1b** (see Ref. [3]), and compounds **1a** and **1c** above.

3.4. Isomerisation of [9,9-$(PPh_3)_2$-9,6,8-$RhS_2B_7H_8$] 2

A solution of [6,6-$(PPh_3)_2$-6,5,9-$RhS_2B_7H_8$] **2** (0.050 g, 0.064 mmol) in benzene (10 cm^3) was heated at reflux for 15 min. The resulting brown solution was filtered through a sintered glass crucible containing tlc-grade silica (7.0 g), using dichloromethane (10 cm^3) as eluent. The filtrate was concentrated under reduced pressure to yield a solid crude product which was washed with hexane (3×5 cm^3) to afford a red, slightly air-sensitive solid tentatively identified as [5,5-$(PPh_3)_2$-5,6,10-$RhS_2B_7H_8$] **3** (0.006 g, 12.0%) (Found: C, 55.8; H, 5.2; S, 8.2. $C_{36}H_{38}B_7P_2RhS_2$ requires C, 55.75; H, 4.95; S, 8.3%). IR: ν_{max} (KBr) 2530(w), 2523(m), 2496(m) (BH) cm^{-1}. ^{11}B and ^1H NMR data for **3** ($CD_3C_6D_5$, 294–297 K) ordered as $\delta(^{11}B)$ [$\delta(^1H)$ of directly attached proton]: +19.3 [+4.80, doublet structure $J(^{31}P-^1H)$ 22 Hz], +17.7 [+4.72], −1.4 [+3.37], −11.5 [+2.43], −15.3 [+2.85], −19.0 [+3.06], −42.1 [+0.87]; $\delta(^1H)(\mu H)$ +0.10 (associated principally with $\delta(^{11}B)$ −15.3 and −19.0); $\delta(^{31}P)$ (219 K, $CD_3C_6D_5$) (a) +38.9 and (b) +28.3, $^1J(^{103}Rh-^{31}P_a)$ 152 Hz, $^1J(^{103}Rh-^{31}P_b)$ 143 Hz, and $^2J(^{31}P_a-^{31}P_b)$ 32 Hz.

3.5. [8,8,10-$(PPh_3)_3$-8-H-10-Cl-8,10,9,7-$Rh_2S_2B_7H_7$] CH_2Cl_2 **4** · CH_2Cl_2

A solution of [$RhCl(PPh_3)_3$] (0.196 g, 0.212 mmol) in dichloromethane (10 cm^3) was added over 3 h to *arachno*-4,6-$S_2B_7H_9$ (0.016 g, 0.106 mmol) in dichloromethane (5 cm^3). The mixture was stirred for 3 d at room temperature during which time it became brown. The mixture was filtered and concentrated under reduced pressure. The crude product was subjected to preparative tlc (CH_2Cl_2–heptane 8:2). The major product ($R_f = 0.45$) was recrystallised from CH_2Cl_2–hexane (6:4) affording orange block crystals of the CH_2Cl_2 solvate of [8,8,10-$(PPh_3)_3$-8-H-10-Cl-8,10,9,7-$Rh_2S_2B_7H_7$], **4**.CH_2Cl_2 (0.046 g, 34.3%). (Found: C, 52.65; H, 4.75. $C_{55}H_{55}B_7Cl_3S_2P_3Rh$ requires C, 52.4; H, 4.4%). IR: ν_{max} (KBr) 2515 m(br), 2495 m(br), 2486 w(sh) (BH), 1992 w (RhH) cm^{-1}. ^{11}B and ^1H NMR data for **4**, ($CDCl_3$, 294–297 K) ordered as $\delta(^{11}B)$[$\delta(^1H)$ of directly attached proton]: +19.4 [+3.96], +15.9 [+5.59], +7.8 [+3.51], ca. +6 [+3.02], −2.8 [+1.97], −6.3 [+2.71], and −25.0 [+1.58]; $\delta(^1H)$(RhH) −11.28, $^1J(^{103}Rh-^1H)$ 21 Hz, $^2J(^{31}P-^1H)$(mean) ca. 14 Hz; $\delta(^{31}P)$ (229 K, $CDCl_3$) (a) +46.9, (b) +32.6, and (c) +6.5 ppm, $^1J(^{103}Rh-^{31}P_a)$ 143 Hz, $^1J(^{103}Rh-^{31}P_b)$ 118 Hz, $^1J(^{103}Rh-^{31}P_c)$ 146 Hz; and $^2J(^{31}P_b-^{31}P_c)$ 10.5 Hz. A minor product

Table 4
Atomic co-ordinates ($\times 10^4$) and equivalent isotropic displacement parameters ($Å^2 \times 10^3$) for **1a** with estimated standard deviations (e.s.d.s) in parentheses. U_{eq} **1a** is defined as 1/3 of the trace of the orthogonalized U_{ij} tensor

	x	y	z	U_{eq}
Pt(9)	1359.74(14)	673.09(14)	2357.28(9)	28.56(6)
B(1)	4020(6)	−2299(5)	2394(4)	57.7(14)
B(2)	3498(7)	−2870(6)	3287(4)	66(2)
B(3)	2706(6)	−2711(5)	2294(4)	58.0(14)
B(4)	2785(5)	−1270(5)	1738(3)	47.6(12)
B(5)	3840(6)	−1424(6)	3351(4)	53.3(13)
S(6)	2436(2)	−1528(2)	4043.0(8)	70.1(4)
B(7)	1676(7)	−2182(6)	3240(4)	59.2(15)
S(8)	962.7(12)	−1170.0(11)	2249.0(8)	51.2(3)
B(10)	3506(5)	−607(5)	2419(3)	41.5(11)
P(1)	2082.9(10)	2240.8(10)	2198.8(6)	36.1(2)
C(111)	847(4)	3924(4)	2070(3)	41.0(9)
C(112)	352(5)	4714(4)	2760(3)	51.2(11)
C(113)	−576(5)	5985(5)	2677(3)	66.3(14)
C(114)	−1019(7)	6485(6)	1899(4)	92(2)
C(115)	−556(8)	5716(6)	1219(4)	110(3)
C(116)	372(6)	4439(5)	1295(3)	78(2)
C(121)	3003(4)	1969(4)	1213(2)	42.2(9)
C(122)	2573(5)	1475(5)	557(3)	51.8(11)
C(123)	3145(6)	1316(5)	−226(3)	65.1(15)
C(124)	4184(6)	1636(6)	−350(3)	76(2)
C(125)	4640(6)	2103(6)	289(4)	81(2)
C(126)	4063(5)	2270(6)	1079(3)	64.9(14)
C(131)	3101(4)	2409(4)	3038(3)	39.3(9)
C(132)	3392(4)	1614(4)	3738(3)	46.5(10)
C(133)	4157(5)	1742(5)	4376(3)	61.4(14)
C(134)	4675(5)	2630(5)	4312(4)	69(2)
C(135)	4367(5)	3438(5)	3631(4)	68(2)
C(136)	3561(5)	3356(5)	2999(3)	55.0(12)
P(2)	−887.8(10)	1980.7(11)	2581.9(7)	41.3(2)
C(211)	−1230(4)	3026(4)	3480(3)	48.2(11)
C(212)	−266(5)	2765(5)	4072(3)	56.5(12)
C(213)	−489(6)	3498(6)	4784(3)	72(2)
C(214)	−1689(7)	4500(7)	4922(4)	99(2)
C(215)	−2673(8)	4754(10)	4345(6)	167(5)
C(216)	−2453(6)	4021(9)	3638(5)	137(4)
C(221)	−1805(4)	1044(4)	2853(3)	47.1(10)
C(222)	−2649(5)	856(6)	2298(4)	65.8(15)
C(223)	−3260(6)	79(7)	2532(5)	83(2)
C(224)	−3044(6)	−510(6)	3290(5)	87(2)
C(225)	−2214(6)	−331(6)	3844(4)	83(2)
C(226)	−1598(6)	459(6)	3634(4)	70(2)
C(231)	−1730(5)	2899(5)	1663(3)	57.8(12)
C(232)	−1245(6)	2366(7)	897(3)	78(2)
C(233)	−1829(8)	2983(8)	157(4)	96(2)
C(234)	−2874(12)	4129(8)	185(5)	158(5)
C(235)	−3387(17)	4648(12)	924(6)	309(13)
C(236)	−2796(12)	4043(10)	1665(5)	241(9)

Table 5
Atom co-ordinates ($\times 10^4$) and equivalent isotropic temperature factors ($Å^2 \times 10^3$) for **4**

	x	*y*	*z*	U_{eq}^a
Rh(8)	6668.7(2)	6952.6(2)	7055.75(14)	19.83(7)
Rh(10)	8362.0(2)	8095.6(2)	8207.05(15)	20.48(8)
P(1)	7090.1(8)	7108.6(7)	5820.3(5)	24.5(2)
P(2)	6928.4(8)	5022.6(8)	7562.8(5)	26.2(2)
P(3)	8814.6(8)	8629.1(7)	9135.5(5)	24.0(2)
Cl	9819.5(8)	6791.7(8)	8320.8(6)	35.7(2)
C(111)	6064(3)	7808(3)	5276(2)	31.8(9)
C(112)	5132(4)	8299(3)	5576(2)	39.5(10)
C(113)	4349(4)	8787(4)	5152(3)	53.6(12)
C(114)	4498(4)	8785(4)	4439(3)	52.1(12)
C(115)	5418(4)	8308(4)	4132(2)	52.1(13)
C(116)	6204(4)	7808(4)	4541(2)	44.6(11)
C(121)	7169(3)	5806(3)	5589(2)	29.7(8)
C(122)	6174(4)	5221(4)	5731(3)	46.3(11)
C(123)	6159(4)	4256(4)	5542(3)	57.0(13)
C(124)	7128(4)	3869(4)	5208(3)	56.3(13)
C(125)	8113(4)	4435(4)	5069(3)	54.3(13)
C(126)	8135(4)	5402(3)	5257(2)	40.9(10)
C(131)	8407(3)	7844(3)	5307(2)	29.2(8)
C(132)	9395(3)	7439(3)	5539(2)	33.0(9)
C(133)	10 401(4)	7989(4)	5186(2)	42.5(10)
C(134)	10 444(4)	8931(4)	4590(2)	50.6(13)
C(135)	9488(4)	9338(4)	4353(2)	50.7(12)
C(136)	8470(4)	8809(3)	4710(2)	41.2(10)
C(211)	6990(3)	4643(3)	8548(2)	29.2(8)
C(212)	5989(4)	4398(3)	9074(2)	39.0(10)
C(213)	6005(4)	4091(3)	9819(2)	45.0(11)
C(214)	7000(4)	4021(3)	10 058(2)	46.0(11)
C(215)	7983(4)	4275(3)	9545(2)	41.2(10)
C(216)	7981(4)	4588(3)	8795(2)	34.7(9)
C(221)	5799(4)	4066(3)	7640(2)	36.0(9)
C(222)	5910(5)	2922(4)	7953(3)	51.4(12)
C(223)	5035(6)	2198(4)	8058(3)	66(2)
C(224)	4038(5)	2589(5)	7892(4)	78(2)
C(225)	3898(5)	3709(5)	7602(4)	76(2)
C(226)	4784(4)	4448(4)	7473(3)	52.2(12)
C(231)	8221(3)	4453(3)	7156(2)	34.0(9)
C(232)	9226(4)	4978(4)	7096(2)	40.6(10)
C(233)	10 238(4)	4556(5)	6818(3)	55.8(13)
C(234)	10 246(5)	3624(5)	6594(3)	70(2)
C(235)	9262(6)	3123(5)	6630(3)	72(2)
C(236)	8246(4)	3534(4)	6902(3)	52.1(12)
C(311)	8931(3)	7596(3)	10 008(2)	27.2(8)
C(312)	9198(3)	7920(3)	10 574(2)	34.1(9)
C(313)	9257(3)	7131(3)	11 244(2)	37.9(9)
C(314)	9029(4)	6024(3)	11 350(2)	39.4(10)
C(315)	8744(4)	5707(3)	10 797(2)	43.3(11)
C(316)	8694(4)	6489(3)	10 124(2)	36.3(9)
C(321)	7979(3)	9672(3)	9465(2)	29.3(8)
C(322)	6986(4)	9324(3)	9977(2)	36.3(9)
C(323)	6260(4)	10 083(4)	10 190(2)	46.2(11)
C(324)	6503(5)	11 203(4)	9890(3)	54.7(13)
C(325)	7483(5)	11 556(3)	9400(3)	51.6(13)
C(326)	8232(4)	10 804(3)	9179(2)	39.5(10)
C(331)	10 208(3)	9240(3)	8700(2)	32.9(9)
C(332)	11 145(4)	8855(4)	8986(2)	44.9(11)
C(333)	12 195(4)	9255(5)	8588(3)	59.5(14)
C(334)	12 320(4)	10 058(5)	7910(3)	67(2)
C(335)	11 389(4)	10 463(4)	7624(3)	61.6(14)
C(336)	10 334(4)	10 052(4)	8011(2)	45.5(11)
B(1)	6397(4)	9533(3)	7338(2)	26.9(9)
B(2)	5651(4)	8712(4)	8194(2)	27.7(9)

Table 5 (continued)

	x	y	z	U_{eq}^{a}
B(3)	5667(4)	8372(3)	7317(2)	26.0(9)
B(4)	7025(3)	8788(3)	6719(2)	24.4(8)
B(5)	7852(4)	9332(3)	7294(2)	24.7(8)
B(6)	6954(3)	9218(3)	8168(2)	24.4(8)
S(7)	5742.7(7)	7104.1(7)	8236.0(5)	24.8(2)
S(9)	8336.0(7)	7948.4(7)	7040.2(5)	23.8(2)
B(11)	6677(3)	7808(3)	8683(2)	22.7(8)
C(1s)	2362(5)	7641(7)	7222(4)	99(3)
CI(1s)	2959(2)	6635(2)	7785(2)	155.0(15)
Cl(2s)	2515(4)	6610(4)	6607(2)	162(2)
CI(3s)	2027(12)	8556(8)	6668(5)	133(5)
CI(4s)	1741(7)	7891(13)	6523(4)	119(4)

[a] $U_{eq} = 1/3 \times$ the trace of the orthogonalised U_{ij} matrix.

(ca. 1%) was isolated as a red, slightly air-sensitive solid. This was shown to be identical (tlc, IR, NMR) with [9,9-$(PPh_3)_2$-*arachno*-9,6,8-$RhS_2B_7H_7$] **2**. (For X-ray diffraction analysis of **4**, see Section 3.6 and Table 3).

*3.6. X-ray diffraction analyses of **1a** and **4***

All crystallographic measurements were made at 200 K on a Stoe STADI4 4-circle diffractometer operating in the ω-θ scan mode using graphite monochromated Mo–K_α radiation ($\lambda = 0.71073$ Å) in the range $3.0 \leq 2\theta \leq 50°$. Both data sets were corrected for absorption empirically using azimuthal ψ-scans. Crystal data and details of data collection and structure refinement are given in Table 3. Both structures were solved by standard heavy atom methods using SHELX-86 [27] and were refined by full-matrix least squares (on F^2) using SHELX-93 [28]. Refinement was essentially the same for both compounds. All non-hydrogen atoms were assigned anisotropic displacement parameters. Phenyl hydrogen atoms were constrained in idealised positions and assigned an isotropic displacement parameter of 1.2 U_{eq} of the parent carbon atom. All cluster associated hydrogen atoms were located on the Fourier difference maps and were freely refined with isotropic displacement parameters. Atomic coordinates are listed in Tables 4 and 5. Thermal parameters, interatomic distances and angles between interatomic vectors have been deposited with the Cambridge Crystallographic Data Centre. Figs. 1 and 2 were prepared with the aid of ORTEP II [29].

Acknowledgements

We thank EOLAS (now FORBAIRT) for support (to MPM), the SERC (now EPSRC) for equipment grants (JDK and MTP), the Academy of Sciences of the Czech Republic, Grant Agency of the Czech Republic (Grant No. 203/97/0060), Johnson Matthey for the generous loan of Pt and Rh salts, Borax Research for support (to JH) and Drs. B. Štíbr and K. Nestor for valuable discussions and cooperation.

References

[1] D. O'Connell, J.C. Patterson, T.R. Spalding, G. Ferguson, J.F. Gallagher, Y. Li, J.D. Kennedy, R. Macías, M. Thornton-Pett, J. Holub, J. Chem. Soc. Dalton Trans. (1996) 3323.
[2] C.-H. Kang, S.-J. Kim, J.-J. Ko, K.-B. Lee, S.O. Kang, Bull. Korean Chem. Soc. 14 (1993) 537.
[3] J.H. Jones, X.L.R. Fontaine, N.N. Greenwood, J.D. Kennedy, M. Thornton-Pett, B. Štíbr, H. Langhoff, J. Organomet. Chem. 445 (1993) C15.
[4] S.O. Kang, L.G. Sneddon, Inorg. Chem. 27 (1988) 3769.
[5] S.O. Kang, P.J. Carroll, L.G. Sneddon, Inorg. Chem. 28 (1989) 961.
[6] G.J. Zimmerman, L.G. Sneddon, J. Am. Chem. Soc. 103 (1981) 1102.
[7] R.P. Micciche, P.J. Carroll, L.G. Sneddon, Organometallics 4 (1985) 1619.
[8] K. Wade, Adv. Inorg. Chem. Radiochem. 18 (1986) 1.
[9] R.E. Williams, Adv. Inorg. Chem. Radiochem. 18 (1986) 64.
[10] K.J. Adams, T.D. McGrath, A.J. Welch, Acta Crystallogr. C 51 (1995) 401.
[11] G.R. Rosair, A.J. Welch, A.S. Weller, Acta Crystallogr. C 52 (1996) 3020.
[12] G. Ferguson, M.C. Jennings, A.J. Lough, S. CoughIan, T.R. Spalding, J.D. Kennedy, X.L.R. Fontaine, B. Štíbr, J. Chem. Soc., Chem. Commun. (1990) 891.
[13] C.W. Jung, M.F. Hawthorne, J. Am. Chem. Soc. 102 (1980) 3024.
[14] M. Bown, X.L.R. Fontaine, H. Fowkes, N.N. Greenwood, J.D. Kennedy, P. Mackinnon, K. Nestor, J. Chem. Soc. Dalton Trans. (1988) 2597.
[15] R. Macías, J. Holub, J.D. Kennedy, B. Štíbr, M. Thornton-Pett, J. Chem. Soc., Chem. Commun. (1994) 2265.
[16] K. Nestor, J.D. Kennedy, M. Thornton-Pett, Inorg. Chem. 31 (1992) 3339.
[17] J.A. Long, T.B. Marder, P.E. Behnken, M.F. Hawthorne, J. Am. Chem. Soc. 106 (1984) 2979.

[18] C.B. Knobler, T.B. Marder, E.A. Mizusawa, R.G. Teller, J.A. Long, P.E. Behnken, M.F. Hawthorne, J. Am. Chem. Soc. 106 (1984) 2990.
[19] J.A. Long, T.B. Marder, M.F. Hawthorne, J. Am. Chem. Soc. 106 (1984) 3004.
[20] J.A. Long, T.B. Marder, M.F. Hawthorne, J. Chem. Soc., Chem. Commun. (1980) 677.
[21] O. Faridoon, N. Dhubhghaill, T.R. Spalding, G. Ferguson, B. Kaitner, X.L.R. Fontaine, J.D. Kennedy, D. Reed, J. Chem. Soc. Dalton Trans. (1988) 2739.
[22] R. Macías, J. Holub, J.D. Kennedy, B. Štíbr, M. Thornton-Pett, W. Clegg, J. Chem. Soc., Dalton Trans. (1997) 149.
[23] J. Plešek, S. Heřmánek, Z. Janousek, Collect. Czech. Chem. Commun. 42 (1977) 785.
[24] J.A. Osborn, G. Wilkinson, Inorg. Synth. 10 (1967) 67.
[25] R. Ugo, F. Cariati, G. La Monica, Inorg. Synth. 2 (1968) 105.
[26] M.J. Church, M.J. Mays, J. Inorg. Nucl. Chem. 33 (1971) 253.
[27] G.M. Sheldrick, Acta Crystallogr. A 46 (1990) 467.
[28] G.M. Sheldrick, J. Appl. Crystallogr. (1993) in preparation.
[29] C.K. Johnson, ORTEP II, Report ORNL-5138, Oak Ridge National Laboratory, TN, USA, (1976).